ARTICLE
PUBLISHED ONLINE: 20 NOVEMBER 2011 | DOI: 10.1038/NCHEMBIO.712

Lysophosphatidic acid directly activates TRPV1 through a C-terminal binding site

Andrés Nieto-Posadas[1], Giovanni Picazo-Juárez[1], Itzel Llorente[1], Andrés Jara-Oseguera[2], Sara Morales-Lázaro[1], Diana Escalante-Alcalde[1]*, León D Islas[2]* & Tamara Rosenbaum[1]*

Since 1992, there has been growing evidence that the bioactive phospholipid lysophosphatidic acid (LPA), whose amounts are increased upon tissue injury, activates primary nociceptors resulting in neuropathic pain. The TRPV1 ion channel is expressed in primary afferent nociceptors and is activated by physical and chemical stimuli. Here we show that in control mice LPA produces acute pain-like behaviors, which are substantially reduced in *Trpv1*-null animals. Our data also demonstrate that LPA activates TRPV1 through a unique mechanism that is independent of G protein–coupled receptors, contrary to what has been widely shown for other ion channels, by directly interacting with the C terminus of the channel. We conclude that TRPV1 is a direct molecular target of the pain-producing molecule LPA and that this constitutes, to our knowledge, the first example of LPA binding directly to an ion channel to acutely regulate its function.

Neuropathic pain can occur after trauma to the nervous system or as a result of diseases such as multiple sclerosis and stroke. It is quite common among the human population and includes symptoms such as continuous burning pain, allodynia and hyperalgesia[1].

The release of certain bioactive lipids contributes to the generation and maintenance of neuropathic pain. However, many of the molecular targets of these molecules remain unknown. Among the molecules for which a role in neuropathic pain has been described is LPA[1].

LPA is found in serum and plasma where it is synthesized mainly by the enzyme autotaxin from precursor lysophospholipids, which in turn are produced by phospholipases A_1 and A_2 (ref. 2). Activated platelets[3] and other cell types such as microglia[4] stimulate LPA production, leading to accumulation of micromolar concentrations of the lipid upon tissue damage[3].

LPA's actions are mediated by G protein–coupled receptors that are specific to LPA (LPA_1–LPA_6)[5] and include the regulation of some ion channels through the activation of pathways downstream of the receptors. Effects of LPA on TRP channels have also been reported[6,7]. For example, high concentrations of LPA (100 μM) stimulate Ca^{2+} mobilization in B-lymphoblast cell lines by regulating the activity of a TRPC channel[6]. Although they do not experimentally demonstrate it, these authors suggest that LPA-induced Ca^{2+} mobilization could be due to direct channel activation as the process was not sensitive to $G_{i/o}$ protein or PLC inhibition[6]. On the other hand, LPA decreases TRPM7 activity in fibroblasts. Because these cells express the LPA_3 (also called EDG-7) receptor, the authors suggest that regulation of TRPM7 by LPA could be due to activation of the G_q-associated signaling pathway[7].

The TRPV1 ion channel is activated by a variety of stimuli such as high temperature[8,9], low pH and pungent compounds[8]. Also, multiple signals that originate from inflammatory processes converge on TRPV1, whose activation in sensory neurons has the final consequence of pain perception.

Because TRPV1 receptors in neurons contribute to hyperalgesia, a connection between TRPV1 and LPA-induced neuropathic pain has been hypothesized[1]. A recent study suggests that pain-related responses in dorsal root ganglion (DRG) neurons from a rat bone cancer model are due to enhanced expression as well as potentiation of the capsaicin and thermal responses of TRPV1 in this disease. These changes in TRPV1 expression and function were suggested to be caused by the activation of the protein kinase Cε (PKCε) pathway downstream of the LPA_1 receptor[10].

Because LPA is linked to painful processes involving pain generation during tissue injury and damage and because other lipids such as PIP_2 are known to interact directly with TRPV1 (refs. 11–13), we set out to determine whether LPA could modify TRPV1 function through direct binding to the channel.

The present study shows that LPA does in fact activate TRPV1 by acting directly on its C-terminal region, and this effect contrasts with all other examples of LPA action on ion channels as it is independent of LPA-receptor activation.

RESULTS

TRPV1 mediates LPA-induced pain behavior

To investigate the acute effects of LPA on TRPV1-mediated pain-related behavior, we assessed capsaicin- and heat-elicited pain behavior by means of the paw-licking and paw-withdrawal assays in control and littermate mice lacking expression of LPP3 (*Lpp3*$^{-/-}$, or *Ppap2b*$^{-/-}$), an enzyme which degrades LPA[14], in the nervous system.

We measured the paw-licking time immediately after injection of the test solution. Whereas both wild-type and *Lpp3*$^{-/-}$ animals showed a greater painful response when injected with capsaicin than did those injected with saline, *Lpp3*$^{-/-}$ mice showed longer paw-licking times after capsaicin injection than did control animals (**Fig. 1a**). When pain behavior was assayed by the paw-withdrawal assay, we also observed a hyperalgesic response to increased temperature in *Lpp3*$^{-/-}$ mice (**Fig. 1b**). As expected, *Trpv1*$^{-/-}$ mice showed no differences with respect to control animals, consistent with what had been demonstrated for low-intensity (5.5 A) stimulation[15] (**Fig. 1b**). To confirm that the painful responses to capsaicin and temperature in the *Lpp3*$^{-/-}$ mouse model are due to TRPV1, we produced *Trpv1*$^{-/-}$ *Lpp3*$^{-/-}$ mice and tested their responses to painful stimuli. These double-knockout animals showed no differences

[1]Departamento de Neurodesarrollo y Fisiología, División Neurociencias, Instituto de Fisiología Celular, Universidad Nacional Autónoma de México, Distrito Federal, México. [2]Departamento de Fisiología, Facultad de Medicina, Universidad Nacional Autónoma de México, Distrito Federal, México. *e-mail: trosenba@ifc.unam.mx or descalante@ifc.unam.mx or islas@liceaga.facmed.unam.mx

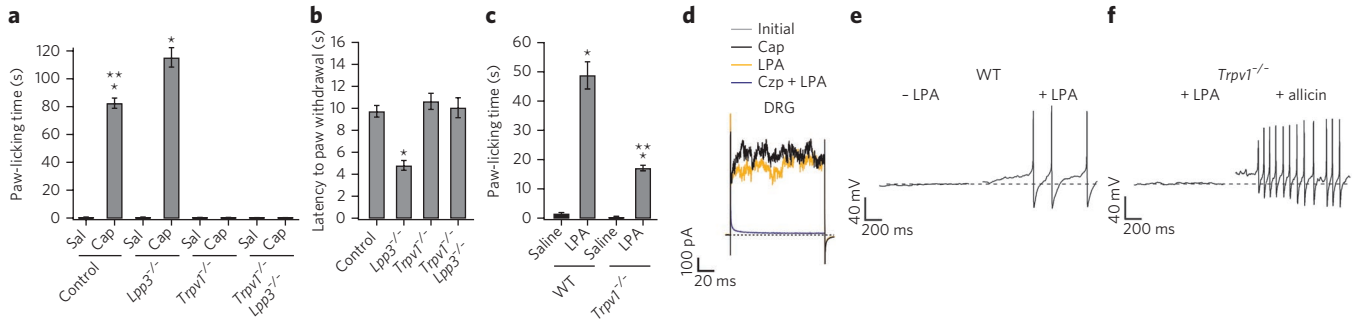

Figure 1 | TRPV1 responds to LPA. (**a**) Paw-licking times for saline and capsaicin, respectively, were: control, 0.8 ± 0.1 s and 82.5 ± 4 s ; *Lpp3*$^{-/-}$, 0.8 ± 0.2 s and 115.42 ± 7 s; *Trpv1*$^{-/-}$, 0.3 ± 0.1 s and 0.4 ± 0.2 s; *Trpv1*$^{-/-}$ *Lpp3*$^{-/-}$, 0.3 ± 0.1 s and 0.4 ± 0.2 s. *P < 0.01 for saline-injected versus capsaicin-injected control and *Lpp3*$^{-/-}$ animals; **P < 0.01 for control mice injected with capsaicin versus *Lpp3*$^{-/-}$ and *Trpv1*$^{-/-}$ mice injected with capsaicin; ANOVA (n = 12). Sal, saline injection; Cap, capsaicin injection. (**b**) Radiant paw-heating (Hargreaves) assay. Latencies were: control, 9.7 ± 0.5 s; *Lpp3*$^{-/-}$, 4.8 ± 0.4 s; *Trpv1*$^{-/-}$, 10.6 ± 0.7 s; *Trpv1*$^{-/-}$ *Lpp3*$^{-/-}$, 10.1 ± 0.9 s. *P < 0.01 *Lpp3*$^{-/-}$ versus all other groups; ANOVA (n = 20). (**c**) Paw-licking times for saline and LPA, respectively, were: control, 1.5 ± 0.3 s and 49 ± 5 s; *Trpv1*$^{-/-}$, 0.4 ± 0.2 s and 17 ± 0.9 s. *P < 0.01 for saline-injected versus LPA-injected animals; **P < 0.01 for control versus *Trpv1*$^{-/-}$ animals injected with LPA; ANOVA (n = 12). (**d**) Representative (n = 5) TRPV1 currents (120 mV) from inside-out DRG neuron membrane patches exposed to capsaicin (Cap, 4 μM), LPA (5 μM, after wash) and LPA (5 μM) and capsazepine (Czp, 30 μM) together. (**e**) Membrane potential in a wild-type DRG neuron with or without 5 μM LPA. (**f**) Membrane potential in a *Trpv1*$^{-/-}$ DRG neuron with LPA and with allicin (200 μM). Resting potential (dashed line) was near −40 mV (n = 8). Group data are reported as the mean ± s.e.m.

in their responses to the injection of saline or capsaicin solutions, and their reaction to changes in temperature (paw withdrawal) were similar to those in *Trpv1*$^{-/-}$ and control mice (**Fig. 1a**,**b**).

Finally, we assayed whether injection of LPA into the paws of wild-type and *Trpv1*$^{-/-}$ mice elicited pain-like behavior. We found that LPA produces a robust (P <0.01) increase in paw-licking time in wild-type animals compared to controls injected with saline (**Fig. 1c**). A nearly 60% decrease in the response to LPA was observed in *Trpv1*$^{-/-}$ mice compared to wild-type animals, although a remnant of the response to LPA was observed in *Trpv1*$^{-/-}$ mice compared to those injected with saline (**Fig. 1c**). Furthermore, we acutely inhibited the TRPV1 channel by injecting the TRPV1 inhibitor capsazepine together with capsaicin or LPA in wild-type mice and measured paw-licking time. Consistently, capsazepine reduced the pain-associated responses to both capsaicin and LPA (**Supplementary Results**; **Supplementary Fig. 1a**).

These data show that more than half of the response to acute LPA delivery is mediated by TRPV1. Thus, the question arises as to how behavioral phenotypes relate to responses at the cellular level. We first sought to answer this question by applying LPA to inside-out membrane patches from dissociated wild-type mouse DRG neurons. LPA elicited currents from membrane patches, and this effect was blocked in all experiments by 30 μM capsazepine applied together with 5 μM LPA (**Fig. 1d**), suggesting that TRPV1 may indeed be a target of LPA.

To establish the physiological role of TRPV1 in the response of DRG neurons to LPA, we performed whole-cell current-clamp recordings in wild-type and *Trpv1*$^{-/-}$ mice. Application of 5 μM LPA to DRG neurons from wild-type mice elicited a depolarization in the range of 7–20 mV and subsequent action potential firing (**Fig. 1e**). DRG neurons that responded to LPA also responded to capsaicin (8 out of 8). In contrast, cells that did not respond to capsaicin did not respond to LPA either (10 out of 10). Although no response to LPA in *Trpv1*$^{-/-}$ neurons was observed, a clear response to allicin (which is also mediated by TRPA1 channels) was present, confirming that LPA was applied to the correct subset of small-diameter DRG neurons (**Fig. 1f**) and indicating that TRPV1 contributes to the electrical response to LPA in DRG neurons.

LPA activates heterologously expressed TRPV1 channels

LPA applied to inside-out patches from TRPV1-transfected HEK293 cells induced robust channel activation at both hyperpolarizing and depolarizing voltages (left and right of **Fig. 2a**, respectively). Furthermore, LPA activated a similar fraction of current with respect to the maximal response to 4 μM capsaicin when applied to patches from TRPV1-expressing HEK cells or wild-type mouse DRG neurons (0.93 ± 0.09 for DRG and 0.93 ± 0.03 for HEK cells; 120 mV, n = 10). In contrast, HEK cells expressing only green fluorescent protein (GFP; **Supplementary Fig. 1b**) did not respond to LPA, and the vehicle used to deliver LPA did not produce TRPV1 channel activation (**Supplementary Fig. 1c**). Moreover, we measured the response to LPA in heterologously expressed TRPV2, TRPV3 and TRPA1 channels, which in many cases colocalize with TRPV1 in native cells, and found that application of LPA to these channels did not produce current activation (**Supplementary Fig. 1d**).

LPA activated a larger fraction of current when it was applied intracellularly than when it was applied extracellularly (**Fig. 2a**,**b**). The time constants of activation (**Fig. 2c**) indicate that LPA is more effective from the inside than from the outside and that LPA applied extracellularly may cross the membrane to act on the intracellular side.

The observed TRPV1 current-voltage relationship was outwardly rectifying with a reversal potential of near 0 mV in the presence of either capsaicin or LPA (**Fig. 2d**). Activation of TRPV1 by LPA occurs in a dose-dependent fashion, with an apparent dissociation constant (K_D) of 754 nM at 120 mV (**Fig. 2e**).

We then probed whether TRPV1 responded to molecules with similar structures to LPA and to molecules that are also substrates or products of the LPP3 enzyme. Intracellular application of 5 μM of glycerol phosphate, oleic acid, lysophosphatidylcholine, diacylglycerol, ceramide-1-phosphate or sphingosine-1-phosphate did not activate TRPV1, but 5 μM phosphatidic acid promoted a small activation of TRPV1 currents (**Supplementary Fig. 1e**).

These data led us to conclude that a robust and specific activation of TRPV1 can be achieved by LPA. We further studied whether LPA could activate TRPV1 through an LPA receptor–independent pathway.

LPA receptors are not involved in TRPV1 activation

So far, our data suggest that LPA acts as a ligand of TRPV1 by promoting a conformational change that leads to the opening of the channel. We then asked whether LPA activates endogenous LPA receptors or whether it interacts directly with the channel.

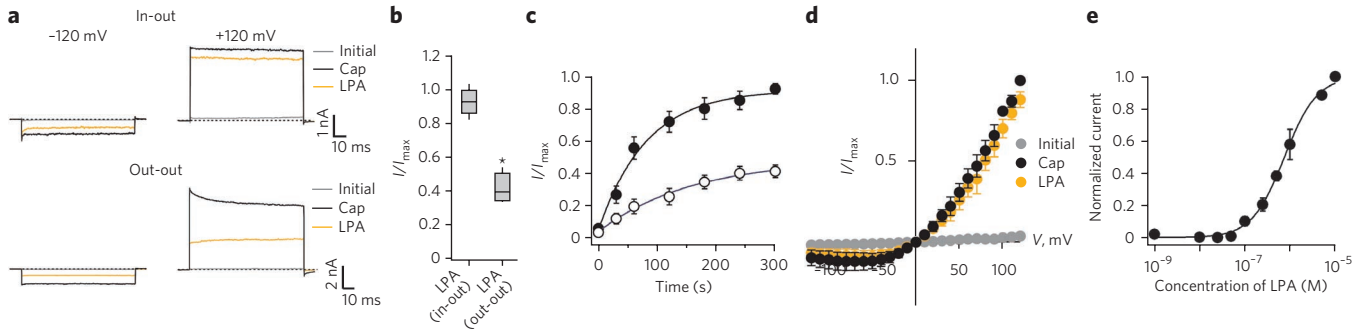

Figure 2 | Heterologously expressed TRPV1 channels respond to LPA. (**a**) Traces shown are representative of five experiments. Currents from inside-out and outside-out HEK cell patches were obtained as in **Figure 1** at −120 mV (left) and 120 mV (right). Patches were first exposed to capsaicin (Cap), washed, and then exposed to LPA. (**b**) Box plot of the fraction of current activated by LPA applied to the intracellular or extracellular face of the channel, normalized to the current with 4 μM capsaicin (120 mV). The horizontal line within each box indicates the median, boxes show the 25th and 75th percentiles, and whiskers show the 5th and 95th percentiles of the data ($n = 6$). *$P < 0.01$, ANOVA. (**c**) Time course of activation by 5 μM LPA in the inside-out (filled symbols) and outside-out (empty symbols) configurations at 120 mV ($n = 5$). Data were fit to a single exponential with time constants 80.5 ± 24 s (inside-out) and 167 ± 77 s (outside-out). LPA application started at $t = 0$ in the abscissa. (**d**) Current-voltage relationships for initial currents (gray), 4 μM capsaicin (black) and 5 μM LPA (orange) after capsaicin was washed off in the inside-out configuration ($n = 5$). (**e**) Dose response for activation by LPA at 120 mV in the inside-out configuration. Smooth curve is a fit with the Hill equation. The K_D value was 754 nM and the slope was 1.2. Owing to seal instability, a single LPA concentration was tested per membrane patch and normalized to the current at 10 μM LPA in the same patch ($n = 5$). Group data are reported as the mean ± s.e.m.

To establish a direct interaction of LPA with the channel, we used the molecule BrP-LPA, which not only closely resembles LPA in structure (**Fig. 3a**) but also is an antagonist of several LPA receptors (LPA_1–LPA_4)[16] and an inhibitor of autotaxin[16].

Unexpectedly, BrP-LPA applied to inside-out membrane patches from DRG neurons (which express LPA_1, LPA_3 and LPA_5)[1,17] and TRPV1-expresing HEK293 cells (which express LPA_1)[18], activated the channel similarly to LPA (**Fig. 3b**). The fraction of current activated by BrP-LPA with respect to the currents activated by 4 μM capsaicin in the same membrane patch at 120 mV was 0.9 ± 0.04 for DRG neurons and 0.91 ± 0.01 for HEK cells. Also, the dose response to BrP-LPA (K_D = 1.1 ± 0.25 μM) was comparable to that for LPA (K_D = 754 nM) (**Fig. 3c**).

Compelled by these results, we studied whether BrP-LPA could mimic LPA's effects at the physiological level. We first examined whether injection of BrP-LPA into the paws of wild-type and *Trpv1*$^{-/-}$ mice mimicked the effects of LPA and found that BrP-LPA produced a significant increase in paw-licking time in wild-type animals compared to saline ($P < 0.01$). The response of *Trpv1*$^{-/-}$ mice to BrP-LPA was only about 20% of that in wild-type animals (**Supplementary Fig. 2**), indicating that BrP-LPA induces a painful sensation that is largely mediated through the activation of TRPV1.

It was also shown that BrP-LPA induces action potential firing in DRG neurons from wild-type mice (**Fig. 3d**, top right) and that these effects are not observed when it is applied to neurons from *Trpv1*$^{-/-}$ mice (**Fig. 3d**, bottom left), although sensitivity to allicin remains (**Fig. 3d**, bottom right).

The data obtained with BrP-LPA suggest that, owing to its structural similarities with LPA, it can activate the channel through the same mechanism as LPA, independently of LPA receptors. To further support our hypothesis, we next performed experiments in which we added both BrP-LPA (BrP-LPA_{out}) to the patch pipette in inside-out patches to act as an antagonist of the LPA receptors and LPA to the intracellular face of the patch (LPA_{in}). Our results show

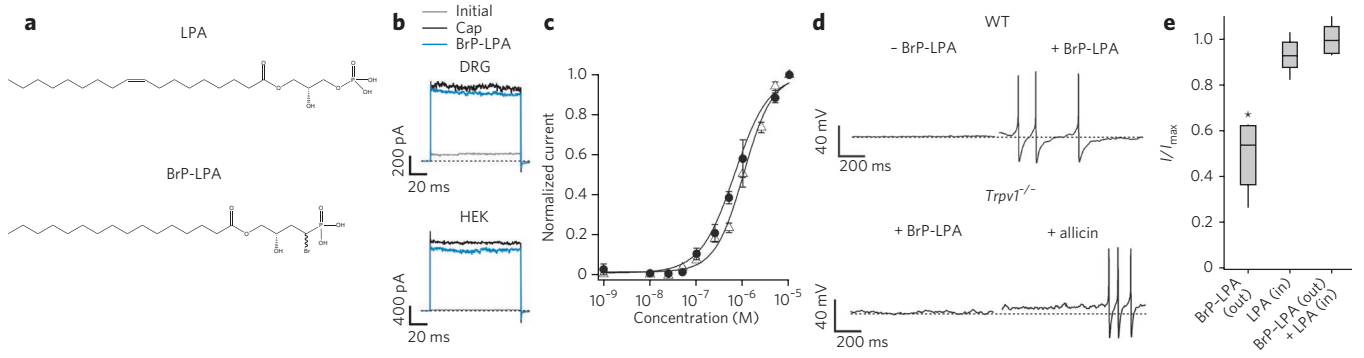

Figure 3 | An antagonist of LPA receptors with a similar structure to LPA activates TRPV1. (**a**) Stick representation of the chemical structures of LPA and BrP-LPA. (**b**) BrP-LPA (5 μM) activates currents in inside-out patches from DRG neurons (top) and HEK cells (bottom) at 120 mV. Representative traces, $n = 8$. Membrane patches were first exposed to 4 μM capsaicin (Cap) and washed, and then BrP-LPA was applied. (**c**) Comparison of BrP-LPA (triangles) and LPA (circles) dose responses at 120 mV obtained from inside-out patches from TRPV1-expressing HEK cells. Data for each patch was normalized to the current at 10 μM of either LPA or BrP-LPA. Smooth lines are fits with the Hill equation. The K_D for BrP-LPA is 1.1 ± 0.25 μM (slope is 1.3 ± 0.21, $n = 5$). (**d**) Membrane potential in a wild-type (WT) DRG neuron before (top left) and during (top right) application of BrP-LPA and in a *Trpv1*$^{-/-}$ DRG neuron during the exposure to BrP-LPA (bottom left) and in the presence of allicin (200 μM; bottom right). Resting membrane potential (dashed lines) was around −40 mV ($n = 9$ per genotype). (**e**) Activation of TRPV1 (120 mV) by external BrP-LPA (5 μM, out) and by internal LPA (5 μM, in) in inside-out patches from HEK cells. Data are normalized to activation with saturating capsaicin. The horizontal lines are as in **Figure 2b**. *$P < 0.01$ with respect to BrP-LPA (out) and LPA (in); ANOVA ($n = 6$). Group data are reported as the mean ± s.e.m.

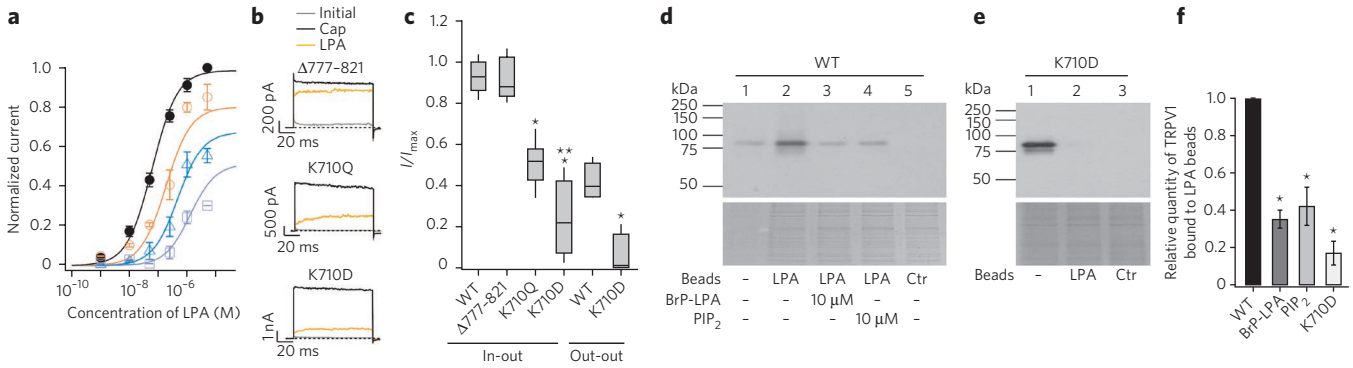

Figure 4 | Interaction site for LPA in the C terminus of TRPV1. (**a**) TRPV1 activation by intracellular LPA after polyK at 120 mV without (filled circles) or with PIP_2 (empty circles, 50 nM; triangles, 100 nM; squares, 200 nM). Curves are fits to **Scheme 1**. (**b**) Representative currents (120 mV, inside-out patches) containing the deletion mutant (Δ777–821) and the mutations K710Q and K710D, activated by 5 μM LPA or 4 μM capsaicin (Cap). (**c**) Fraction of current activated by intracellular LPA in wild-type and mutant TRPV1 channels (normalized to 4 μM capsaicin) and extracellular LPA in K710D mutants and wild type (n = 6–10). Horizontal lines are as in **Figure 2b**. *P < 0.01 versus wild-type (WT) and **P < 0.05 versus $TRPV1^{K710Q}$; ANOVA test. (**d**) TRPV1 interaction with LPA-coated beads. Lane 1, input (1 μg); 2, TRPV1 bound to LPA beads; 3 and 4, competition of BrP-LPA and PIP_2 for beads, respectively; 5, interaction with control beads. Lanes 2, 3, 4 and 5 contained 30 μg of membrane protein. Lower panel shows Coomassie blue–stained supernatant fraction. (**e**) Interaction of the K710D mutant with LPA-coated beads. Lane 1, the input (5 μg) of the K710D mutant; 2, pull-down of $TRPV1^{K710D}$ with LPA beads; 3, control beads. Lanes 2 and 3 contain 60 μg of membrane protein. Lower panel as in **d**. (**f**) Bar graph for the relative quantity of pulled-down TRPV1 with LPA beads from experiments as in **d** and **e**. Normalized values with respect to wild-type were: BrP-LPA = 0.35 ± 0.04; PIP_2 = 0.42 ± 0.09 and K710D = 0.17 ± 0.06. n = 4–6 for each case. *P < 0.01 versus wild-type; ANOVA test. Group data are reported as the mean ± s.e.m.

that the magnitude of the currents activated by LPA under these conditions was not different from the magnitude of those activated by intracellular LPA alone (**Fig. 3e**). In fact, extracellular BrP-LPA ($BrP\text{-}LPA_{out}$) could sustain current activation as effectively as extracellular LPA at the same concentration (**Figs. 2b** and **3e**).

The LPA_5 receptor, which is activated by BrP-LPA[19], is expressed in DRG neurons[17] and HEK cells (**Supplementary Fig. 3a**). To rule out any contributions of LPA_5 to our electrophysiological recordings, we determined whether the LPA_5 agonist farnesyl-pyrophosphate (FPP) could activate the TRPV1 channel. **Supplementary Figure 3b** shows that FPP was incapable of eliciting current activation in TRPV1-expressing HEK cells both in the inside-out and on-cell configurations, in accordance with a previous study that also showed a lack of effect of FPP on TRPV1[20]. However, FPP activated heterologously expressed TRPV3 (**Supplementary Fig. 3c**), as previously reported[20]. These data indicate that LPA is able to promote TRPV1 channel function through a mechanism independent of the activation of LPA receptors 1–5 (**Supplementary Fig. 3d**).

To further rule out the involvement of any LPA receptor in TRPV1's response to this lipid, we treated TRPV1-transfected HEK cells with inhibitors of the G protein–coupled signaling pathways that are associated with activation of LPA receptors. We used the inhibitors of phospholipase C (U73122; ref. 21); Rho-associated protein kinases and PKC (Y-27632; ref. 22); G_i, G_o and G_t proteins (pertussis toxin, PTX[23]); the βγ subunit of G proteins (C terminus of β-adrenergic kinase 1, Ctr-βARK1; ref. 24); and adenylyl cyclase (2′,5′-dideoxyadenosine or 2′,5′-dd-Ado[25]). We found that none of the treatments precluded current responses to extracellular LPA in on-cell recordings and that the responses were in fact indistinguishable from those elicited in untreated cells (**Supplementary Fig. 3e**), leading us to conclude that LPA receptor activation is not necessary for TRPV1 activation by LPA.

Because a recent study in an induced bone cancer model shows that LPA might regulate expression and activity of TRPV1 through a PKC-dependent pathway[10], we tested this possibility in our system. Incubation of TRPV1-transfected HEK293 cells with the PKC inhibitors Y27632 (ref. 22) and BIM I[26] had no effect on LPA activation of TRPV1 in on-cell experiments (**Supplementary Fig. 4a**). PKCε has been reported to be responsible for LPA-induced potentiation of TRPV1 by heat and capsaicin[10]. To assess whether this was a possibility, we performed experiments in which we transfected HEK293 cells with a plasmid containing either a dominant-negative form of PKCε[27] or the wild-type functional version of PKCε[27] together with TRPV1. Overexpression of either form of PKCε did not have an effect on acute activation of TRPV1 by LPA (**Supplementary Fig. 4b**,**c**).

To further establish the lack of a role for PKCε in our model, we used the specific inhibitor $εV_{1\text{-}2}$ (ref. 10) in whole-cell recordings of DRG neurons to determine whether blockage of this pathway precluded activation of TRPV1. All DRG neurons tested for TRPV1 activation by LPA responded irrespectively of the presence of the specific inhibitor $εV_{1\text{-}2}$ applied in the recording pipette, leading to the conclusion that PKCε is not necessary for acute LPA activation of TRPV1, contrary to what was previously suggested[10] (**Supplementary Fig. 4d**). Nonetheless, in accordance to the study mentioned above, we, too, observed a potentiating effect of LPA on capsaicin currents (**Supplementary Fig. 5a**).

So far, our data demonstrate that LPA promotes its effects on TRPV1 independently of LPA receptors, most likely through a direct interaction with the channel.

Interaction site for LPA in the C terminus of TRPV1

Some proteins known to interact with LPA share binding sites with other lipids such as PIP_2 (refs. 28,29). PIP_2 binds directly to TRPV1 and enables the channel's response to capsaicin without activating it[13]. Conversely, depletion of PIP_2 results in decreased channel activity induced by capsaicin[30,31] (**Supplementary Fig. 5b**).

To determine whether LPA could share a binding site with PIP_2, we performed a competition assay. Using an established approach[7,13], we constructed a dose-response curve for activation by LPA by first removing endogenous PIP_2 with the scavenger polylysine (polyK) and then applying different concentrations of LPA. Interestingly, removal of PIP_2 with polyK did not preclude TRPV1 activation by LPA (**Fig. 4a**), although polyK did scavenge LPA (**Supplementary Fig. 5c**,**d**). Moreover, the data in **Figure 4a** show that the dose-response curve for TRPV1 activation by LPA after treatment with polyK is shifted to the left, and the K_D of TRPV1 for LPA is lower than that measured in the presence of endogenous PIP_2 (71 nM versus 754 nM). We then repeated the experiment described above but

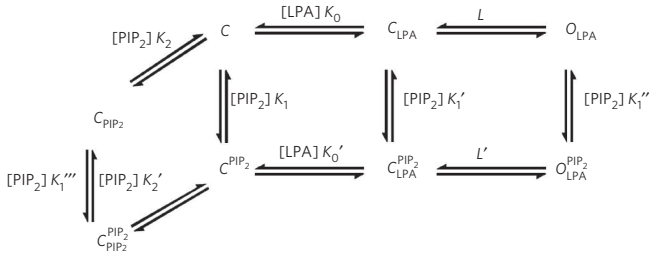

Scheme 1 Model for TRPV1 modulation by LPA and PIP_2. The model considers a shared PIP_2- and LPA-binding site for which both lipids compete and a second PIP_2 binding site from which PIP_2 modulates LPA binding and channel gating. At equilibrium, the relative current is given by

$$\frac{I}{I_{max}} = \frac{[LPA]K_0L(1+[PIP_2]K_1'')}{1+[LPA]K_0+[LPA][PIP_2]K_0'K_1'+[PIP_2](K_1+K_2)+[PIP_2]^2K_1K_2'+[LPA]K_0L(1+[PIP_2]K_1'')}$$

where [LPA] and [PIP_2] are the lipid's molar concentrations, K_0, K_0', K_1, K_1', K_1'', K_1''', K_2 and K_2' are association constants between the channel and LPA or PIP_2, and L and L' are equilibrium constants for channel gating. In the C_X^Y notation used here, C denotes closed states, O denotes open states, X denotes ligand occupancy of the shared LPA- and PIP_2-binding site and Y denotes ligand occupancy of the PIP_2-only site. This equation was used to fit the data in **Figure 4a** with following parameters: $K_0 = 2.3 \times 10^5\ M^{-1}$, $K_0' = 17.5 \times 10^6\ M^{-1}$, $K_1 = 4.2 \times 10^6\ M^{-1}$, $K_1' = 3.2 \times 10^8\ M^{-1}$, $K_1'' = 3.2 \times 10^4\ M^{-1}$, $K_1''' = 5.5 \times 10^8\ M^{-1}$, $K_2 = 1.7 \times 10^6\ M^{-1}$, $K_2' = 2.2 \times 10^8\ M^{-1}$, $L = 70$ and $L' = 7 \times 10^{-3}$.

applied LPA together with different concentrations of DiC8-PIP_2, a water-soluble form of PIP_2 (**Fig. 4a** and **Supplementary Fig. 5c**,**d**).

These data show that with increasing PIP_2 concentrations, the apparent affinity for LPA is diminished, as evidenced by a rightward shift in the dose responses for activation by LPA (**Fig. 4a**). However, the magnitude of the maximum response to LPA was also decreased in the presence of PIP_2.

In a simple competition, the LPA dose-response curves are expected to be shifted to the right upon increasing PIP_2 concentrations without a change in the maximum response (that is, there should be a concentration of LPA than can actually displace PIP_2 from the binding site). Our results can be explained by the allosteric effect of PIP_2 on the binding of LPA to TRPV1 together with the competition between PIP_2 and LPA for the same binding region (described further in Discussion; **Fig. 4a**, **Scheme 1**).

As LPA is a negatively charged molecule, we mutated sites proposed to interact with PIP_2 because these contain positively charged residues that could bind LPA. We first removed residues 777–821 in the C terminus, which contains several positively charged amino acids[32], and tested the effects of LPA. LPA activated this deletion mutant similarly to its activation of wild-type channels (**Fig. 4b**,**c**). We then mutated another positive residue in the C terminus, Lys710 (ref. 11). A charge-neutralization mutation (K710Q) produced a channel with a markedly decreased (nearly 50%) response to LPA (**Fig. 4**,**c**) that retained normal capsaicin activation (**Supplementary Fig. 6a**). We then explored the effects of the charge-reversal mutation K710D and found that it also behaved similarly to the wild type in its response to capsaicin (**Supplementary Fig. 6a**), but nearly 80% of the response of the channel to LPA (**Fig. 4b**,**c**) and to BrP-LPA (**Supplementary Fig. 6b**) was abolished. Moreover, when we applied LPA to the K710D mutant from the extracellular side, we found that a smaller fraction of current was activated compared to when extracellular LPA was applied to the wild-type channel. These data indicate that the intracellular Lys710 residue accounts for most of the effects of LPA on TRPV1 (**Fig. 4c**).

Finally, we took a biochemical approach to confirm a direct interaction between TRPV1 and LPA. Using membrane-protein extracts from HEK293 cells transfected with TRPV1, we performed pull-down experiments to test for LPA-TRPV1 interactions with agarose beads bound to LPA (LPA beads).

The LPA beads bound to the TRPV1 channel significantly ($P < 0.01$) more than control beads without the lipid (**Fig. 4d** and **Supplementary Fig. 7a**), as evidenced by the differences in signal intensity of the TRPV1 band (molecular mass of 85–90 kDa[33]), suggesting that TRPV1 physically interacts with LPA.

So far, these results constitute strong evidence for direct interaction of the channel with LPA. To further support this hypothesis, we decided to explore whether BrP-LPA, which seems to activate TRPV1 through the same mechanism as LPA, was able to diminish channel binding to the LPA beads by competing for the same site. As expected, preincubation of membrane-protein extracts with BrP-LPA reduced binding of TRPV1 to LPA beads and decreased the intensity of the TRPV1 signal on the immunoblot (**Fig. 4d** and **Supplementary Fig. 7a**).

Furthermore, we used this assay to test for competition of the LPA-beads with PIP_2 for binding to TRPV1. The data in **Figure 4d** show that PIP_2 can diminish the signal associated with LPA-bead binding to TRPV1, indicating that PIP_2 antagonizes LPA at the level of channel binding, probably in competition for a binding site.

Finally, we tested for a correlation between the lack of a functional response of the K710D mutant to LPA and the effects of this mutation on the binding of TRPV1 to the LPA beads. We found that this charge-reversal mutant bound to LPA beads very poorly (**Fig. 4e** and **Supplementary Fig. 7b**). A quantitative analysis of our pull-down assays is presented in **Figure 4f**. The data obtained strongly suggest that LPA binds to the TRPV1 channel and that the Lys710 site is important for LPA binding.

DISCUSSION

Many TRP channels play a pivotal role in the detection of environmental stimuli and pain perception. TRPV1 is implicated in several painful processes, and interactions of this channel with some exogenous pain-producing molecules have been demonstrated[8]. However, our knowledge of the molecular mechanisms of TRPV1 activation by substances released during injury or inflammation remains scarce. LPA has an important role in the development of neuropathic pain[34]. It has been suggested that during the development of neuropathic hyperalgesia, an upsurge in LPA production occurs, leading to myelinated Aδ fiber hypersensitivity that is partially due to upregulation of TRPV1 (ref. 35). Despite this clear proposition, to date, the role of TRPV1 in LPA-induced chronic pain had remained unclear and, in the case of acute pain, unaddressed.

Actions of LPA on ion channels in peripheral nociceptors have been classically circumscribed to the activation of receptor-mediated signaling pathways[21,36]. Our work constitutes the first study to show a direct and physiologically relevant interaction of an ion channel and LPA, and several lines of evidence presented here support this

idea: (i) BrP-LPA, an antagonist of LPA receptors structurally similar to LPA, activates TRPV1; (ii) inhibitors of the G protein–coupled receptor signaling pathways, which are coupled to LPA-receptor activation, do not preclude actions of LPA on TRPV1; (iii) blockers and dominant-negative forms of PKC and PKCε, previously linked to activation of TRPV1 by LPA, had no effects on both a heterologous expression system and the native DRG neurons; (iv) TRPV1 interacts directly with LPA, as shown by pull-down assays; and (v) mutation of a charged residue in the C terminus of TRPV1 considerably reduces the effects of LPA and BrP-LPA on the channel and eliminates interactions of the channel with LPA in pull-down assays.

A recent study shows that application of a LPA receptor antagonist attenuates thermal hyperalgesia in a rat model of bone cancer. On the basis of this observation, the authors propose a possible role for the regulation of TRPV1 activity by LPA receptor–mediated signaling pathways, specifically PKCε-dependent pathways[10]. However, we did not observe any role of PKCε for TRPV1 activation by LPA in our experiments. In that respect, the study mentioned above shows experiments performed in a model involving the induction of a cancerous process[10], which complicates interpretation of the results. For example, after only 9 days of introducing cancerous cells to the animal model, the authors were able to observe an increase in paw-withdrawal latency when animals were injected with an LPA_1-receptor antagonist[10]. Cancerous processes are accompanied by inflammatory responses, and bone cancers induce demyelination of sensory fibers, a phenomenon that leads to hyperalgesic responses[37]. Furthermore, most osteolytic tumors cause extracellular acidification[38], which may potentiate TRPV1 activity independently of LPA. The hyperalgesic responses observed in ref. 10 could also be due to the already-demonstrated overexpression of TRPV1 in some cancerous processes[10,39] and the potentiated response of the channel to inflammatory mediators known to modulate its activity through the activation of PKC-dependent pathways[8]. We were able to reproduce the potentiating effect of LPA on the TRPV1 capsaicin response reported in ref. 10, but we conclude that this is just an additive effect of two agonists binding to different regions in the channel.

Other studies in which LPA was delivered intraplantarly to mice show that LPA-induced pain responses can be blocked either by injection of LPA together with PTX or by inhibition of LPA_1 expression[40], suggesting that acute peripheral nociceptor responses to LPA depend on the $G_{i/o}$-coupled LPA_1 receptor. These data seem to exclude a major role for direct activation of TRPV1 by LPA in nocifensive behavior generation.

However, different lines of evidence from our experiments point to the contrary. First, our findings show that TRPV1, which is expressed in peripheral nociceptors, is robustly and directly activated by LPA and BrP-LPA, an inhibitor of LPA_1. Second, BrP-LPA produced similar responses to LPA in our behavioral assays and triggered action-potential firing in cultured DRG neurons, indicating that LPA_1 is not essential for the generation of acute pain responses triggered by LPA. Furthermore, the experimental recordings in ref. 40 were performed after prolonged nociceptor stimulation, which favors TRPV1 channel desensitization. The resulting decrease in TRPV1 channel responsiveness to agonists could have obscured its role in the acute response to LPA.

Moreover, the authors in ref. 40 measured pain responses after LPA and PTX were injected together into the paws of mice and showed that, after only 20 min, PTX was able to produce a decrease in the pain response. The pain-related behavior up to 10 min was the same as the control response obtained in the presence of only LPA, consistent with our observations that LPA causes acute pain partly through TRPV1. Responses at longer LPA exposures could indeed stem from other molecular entities such as LPA_1. It is certain that it is not only a single effector that controls the responses to LPA and other painful stimuli. Our own data show that there are residual responses in the behavioral assay in the TRPV1-null mice after LPA and BrP-LPA injection (**Fig. 1c** and **Supplementary Fig. 2**) that could be due to other molecules affected by the activation of the signaling pathways resulting from LPA-receptor activation, such as LPA_1 or LPA_5.

With regard to the nature of the interaction between channel and lipid, we established that one of the proposed PIP_2 binding sites in the TRPV1 channel, the residue Lys710 (ref. 11), in fact mediates binding of LPA. This interaction possibly occurs partly through an electrostatic mechanism, as a charge neutralization of this site is not as effective as a charge reversal in precluding LPA activation of TRPV1, and probably also through hydrophobic interactions with the acyl chain of LPA.

Lys710 is located in the region that constitutes the TRP-like domain and is also a tetramerization domain for the protein, and deletions in this region hinder the formation of stable multimers[41]. From our experiments with the K710D mutant, we observed that nearly 80% (but not all) of the response to LPA is abolished. It is possible that other residues also participate in the stabilization of LPA binding to TRPV1. To determine this, we mutated other charged residues in this region, including the nearby Arg701 residue as well as Lys694, Lys698, Lys714 and Arg718. However, none of these mutations produced functional channels. The deletion of a stretch of residues in the distal C terminus, previously reported as important for interactions of TRPV1 with PIP_2 (ref. 32), also had no effect on LPA activation of TRPV1.

Regarding the effects of PIP_2 on the channel's response to LPA, we found that PIP_2 reduces the apparent affinity of the channel for LPA. This is observed as a reduction in both the affinity for LPA obtained from the dose-response curves and the channel binding to LPA beads when PIP_2 is present. Moreover, the presence of PIP_2 also reduces the channel's maximum response to LPA. The effects on apparent affinity could be due to overlapping binding sites for LPA and PIP_2. However, the reduction in the maximal response indicates that a complex allosteric interplay between LPA and PIP_2 might be taking place. Allosteric modulation of the effects of LPA by PIP_2 is not surprising because PIP_2 allosterically modulates the activation of TRPV1 by capsaicin through binding to several sites throughout the channel. In accordance with this interpretation, we produced a model that considers the competition between LPA and PIP_2 for a site in the channel and the allosteric modulation of LPA binding and channel activation through a second PIP_2 binding site (**Fig. 4a** and **Scheme 1**) and found that it satisfactorily accounts for our data.

How does LPA reach its intracellular binding site under physiological conditions? Intracellular LPA is produced mainly as a precursor of membrane phospholipids in the endoplasmic reticulum and mitochondria. The role for the intracellular LPA pool in cell signaling is not clear. Moreover, its effects on intracellular protein receptors such as PPARγ have been ascribed to the extracellular LPA pool, which finds its way into the cell[42]. Although LPA is present in serum at elevated concentrations, the large protein-bound fraction thereof reduces its effective concentration and its potency to activate some of its receptors[43]. Nonetheless, autotaxin associates with integrins[44] in the plasma membrane and contains a hydrophobic channel connected with the active site, which has a flat entrance that could interact with the membrane. On the basis of these findings, it has been proposed that the enzyme could locally deliver LPA, which could elevate the local concentration of the lipid above the maximal reported values for serum LPA[45,46]. Although the flip-flop rate of LPA is unknown, activation of the nuclear PPARγ receptor by extracellular LPA has been shown to be physiologically relevant, suggesting that efficient mechanisms of transbilayer movement of LPA exist. The apparent lack of a delay in channel activation by extracellular LPA in our experiments also indicates that the rate of transbilayer movement of LPA is comparable to the rate of channel activation. Also, these mechanisms for extracellular delivery of LPA do not preclude the possible role of intracellularly synthesized LPA in TRPV1 activation.

In this study we provide strong evidence that TRPV1 is directly activated by LPA, a mechanism that further broadens our understanding of how bioactive lipids act on nociceptors to produce and maintain pain. Our results also suggest a broader role of LPA in acute pain responses such as angina pectoris (the atherosclerotic plaque that produces ischemia contains high concentrations of LPA[47]), bites from animals whose venoms contain enzymes that convert lysophosphatidylcholine to LPA (such as those of the brown recluse or violin spider, *Loxosceles reclusa*[48]) or snake venoms that contain phospholipase A_2 (ref. 49), which also catalyzes the formation of LPA.

METHODS

Mice strains and genotyping. C57BL/6J and *Trpv1*$^{-/-}$ mice were obtained from The Jackson Laboratory (Bar Harbor, Maine). Animals with neural inactivation of *Ppap2b* (*Ppap2b*$^{tm3Stw/tm3Stw}$; Nes-cre mouse line), named here for simplicity *Lpp3*$^{-/-}$, were obtained from our animal facility[14]. *Lpp3*$^{-/-}$ and *Trpv1*$^{-/-}$ animals were mated to obtain double-mutant mice. The C57BL/6J mice were used as controls for the behavioral experiments on *Trpv1*$^{-/-}$ mice, and *Ppap2b*$^{tm3Stw/tm3Stw}$ littermates were used as controls for *Lpp3*$^{-/-}$ and *Trpv1*$^{-/-}$ as well as *Lpp3*$^{-/-}$ mouse experiments. For PCR genotyping of complete *Ppap2b* Cre-mediated recombination as well as *Trpv1*$^{-/-}$ and Cre genotyping, we followed previously described methods[14,15].

Pain-related behavioral assays. 10 µl of either saline solution (0.9% w/v of NaCl) or capsaicin (2.8 µg), LPA (4.1 µg), BrP-LPA (3 µg) or capsazepine (2.2 µg) diluted in saline was injected intraplantarly using a 30-gauge needle, and paw-licking behavior was quantified for 10 min immediately after injection. Animals were handled according to institutional standards from the US National Institutes of Health (NIH). Thermal hyperalgesia was assessed by measuring paw withdrawal latency to radiant heat (University of California San Diego Thermal Paw stimulator) as previously described[15]. A current of 5.5 A was applied to each of the hind paws, and the mean of the withdrawal latencies was defined as paw-withdrawal latency.

Mutagenesis. Point mutations and deletions in the rTRPV1 channel were constructed by a two-step PCR method as previously described[50].

DRG and HEK293 cell culture and recording. DRG neurons were obtained following previously described procedures[12]. HEK293 cells were transfected with wild-type and mutant pcDNA3-rTRPV1, pIRES-GFP (BD Biosciences) and with FLAG.PKCepsilon (Addgene plasmid 10795) or FLAG.PKCepsilon.K/W (Addgene plasmid 10796) with JetPei (Polyplus Transfection). Currents were recorded using the inside-out, outside-out and on-cell configurations of the patch-clamp technique[44]. Solutions were changed with a RSC-200 rapid solution changer (Molecular Kinetics). The solution for both inside-out and on-cell recording under isometric conditions comprised 130 mM NaCl, 3 mM HEPES (pH 7.2) and 1 mM EDTA. Capsazepine and capsaicin were diluted in DMSO and ethanol, respectively. Experiments were performed at 24 °C. Mean current values for LPA were measured after channel activation had reached the steady state (~5 min). Currents were obtained using voltage protocols with a holding potential of 0 mV. Steps from −120 to 120 mV were applied for 100 ms, and then the voltage was returned to 0 mV. Currents were low-pass filtered at 2 kHz, sampled at 10 kHz with an EPC 10 amplifier (HEKA Elektronik), and plotted and analyzed with Igor Pro (Wavemetrics Inc.).

Whole-cell currents from DRG neurons were recorded following previously described methods[10]. Action potentials were recorded in the whole-cell configuration from acutely dissociated DRG neurons from wild-type or *Trpv1*$^{-/-}$ mice following methods previously described[44]. The membrane potential was recorded continuously, and LPA or allicin were applied directly to the bath solution.

LPA binding assay. Plasma membrane proteins from HEK293 cells transfected with wild-type TRPV1 or the K710D mutation were biotinylated and extracted using the Pierce cell-surface protein isolation kit according to manufacturer instructions with minor modifications (elution of proteins was performed with non-ionic detergents). Total membrane-protein extracts were incubated with LPA or control beads (Echelon Biosciences) for 3 h at 4 °C and were washed five times with binding buffer containing 0.5% Igepal (Sigma). To ensure equal protein input between conditions, proteins in equivalent volumes of the first supernatant (50 µl) were separated by SDS-PAGE and analyzed by Coomasie blue staining of the gel.

For competition assays, protein extracts were incubated with 10 µM BrP-LPA or DiC8-PIP_2 prior to the addition of LPA or control beads. Pulled-down protein from each sample was eluted from the beads by adding an equal volume of 2× Laemmli sample buffer to beads and heating to 95 °C for 5 min. Eluted proteins were separated by SDS-PAGE and analyzed by immunoblotting using a TRPV1-specific antibody (Alomone Labs). For each experiment, a small sample of the total membrane-protein extract was loaded into the gel as a positive control of TRPV1 protein expression (lane 1 in **Fig. 4d,e**). Immunoblots were developed by enhanced chemiluminesence, and densitometric analysis was done using ImageJ software (NIH) and expressed as relative amounts of protein versus the amount of TRPV1 bound to LPA beads.

Lipids and polylysine. LPA (Avant Polar Lipids or Sigma) and BrP-LPA (Echelon) dilutions were freshly prepared every day and sonicated in a cold bath. Stock solutions of LPA (10 mM) were prepared in DMEM with 1% fatty acid–free BSA (Roche), and BrP-LPA was prepared in water. Stock solutions were sonicated and frozen before use. DiC8-PIP_2 (Echelon Biosciences) was solubilized in recording solution and frozen at −20 °C. Phosphatidic acid and diacylcglycerol (both from Avanti Polar Lipids) were diluted in chloroform, glycerol phosphate in water, sphingosine-1-phosphate in DMEM, oleic acid in ethanol and ceramide-1-phosphate (Avanti Polar Lipids) and lysophosphatidylcholine in chloroform:methanol (1:1), and a final concentration of 5 µM was obtained by diluting in recording solution. FPP (Echelon Biosciences) was used at a concentration of 1.5 µM.

Experiments to determine the effects of PIP_2 on TRPV1 activation by LPA were performed following previously established methods[13]. Briefly, we applied polyK (15 µg ml^{-1}) to inside-out membrane patches and then measured the response to different concentrations of LPA in the absence and presence of different concentrations of PIP_2 to construct a dose-response curve. Data were normalized to the maximal current obtained in the presence of 5 µM LPA without PIP_2.

Statistical analysis. Statistical comparisons were made with a one-way ANOVA test. $P < 0.05$ was considered statistically significant. Group data are reported as the mean ± s.e.m. Additional experimental procedures can be found in **Supplementary Methods**.

Received 4 April 2011; accepted 29 August 2011;
published online 20 November 2011; corrected online 15 June 2012

References

1. Inoue, M. *et al.* Initiation of neuropathic pain requires lysophosphatidic acid receptor signaling. *Nat. Med.* **10**, 712–718 (2004).
2. Okudaira, S., Yukiura, H. & Aoki, J. Biological roles of lysophosphatidic acid signaling through its production by autotaxin. *Biochimie* **92**, 698–706 (2010).
3. Lin, M.E., Herr, D.R. & Chun, J. Lysophosphatidic acid (LPA) receptors: signaling properties and disease relevance. *Prostaglandins Other Lipid Mediat.* **91**, 130–138 (2010).
4. Ma, L., Nagai, J. & Ueda, H. Microglial activation mediates de novo lysophosphatidic acid production in a model of neuropathic pain. *J. Neurochem.* **115**, 643–653 (2010).
5. Chun, J., Hla, T., Lynch, K.R., Spiegel, S. & Moolenaar, W.H. International Union of Basic and Clinical Pharmacology. LXXVIII. Lysophospholipid receptor nomenclature. *Pharmacol. Rev.* **62**, 579–587 (2010).
6. Roedding, A.S., Li, P.P. & Warsh, J.J. Characterization of the transient receptor potential channels mediating lysophosphatidic acid-stimulated calcium mobilization in B lymphoblasts. *Life Sci.* **80**, 89–97 (2006).
7. Runnels, L.W., Yue, L. & Clapham, D.E. The TRPM7 channel is inactivated by PIP(2) hydrolysis. *Nat. Cell Biol.* **4**, 329–336 (2002).
8. Jara-Oseguera, A., Simon, S.A. & Rosenbaum, T. TRPV1: on the road to pain relief. *Curr. Mol. Pharmacol.* **1**, 255–269 (2008).
9. Yao, J., Liu, B. & Qin, F. Modular thermal sensors in temperature-gated transient receptor potential (TRP) channels. *Proc. Natl. Acad. Sci. USA* **108**, 11109–11114 (2011).
10. Pan, H.L., Zhang, Y.Q. & Zhao, Z.Q. Involvement of lysophosphatidic acid in bone cancer pain by potentiation of TRPV1 via PKCε pathway in dorsal root ganglion neurons. *Mol. Pain* **6**, 85 (2010).
11. Brauchi, S. *et al.* Dissection of the components for PIP2 activation and thermosensation in TRP channels. *Proc. Natl. Acad. Sci. USA* **104**, 10246–10251 (2007).
12. Stein, A.T., Ufret-Vincenty, C.A., Hua, L., Santana, L.F. & Gordon, S.E. Phosphoinositide 3-kinase binds to TRPV1 and mediates NGF-stimulated TRPV1 trafficking to the plasma membrane. *J. Gen. Physiol.* **128**, 509–522 (2006).
13. Ufret-Vincenty, C.A., Klein, R.M., Hua, L., Angueyra, J. & Gordon, S.E. Localization of the PIP2 sensor of TRPV1 ion channels. *J. Biol. Chem.* **286**, 9688–9698 (2011).
14. Escalante-Alcalde, D., Sanchez-Sanchez, R. & Stewart, C.L. Generation of a conditional Ppap2b/Lpp3 null allele. *Genesis* **45**, 465–469 (2007).
15. Caterina, M.J. *et al.* Impaired nociception and pain sensation in mice lacking the capsaicin receptor. *Science* **288**, 306–313 (2000).
16. Jiang, G. *et al.* α-substituted phosphonate analogues of lysophosphatidic acid (LPA) selectively inhibit production and action of LPA. *ChemMedChem* **2**, 679–690 (2007).
17. Oh, D.Y. *et al.* Identification of farnesyl pyrophosphate and N-arachidonylglycine as endogenous ligands for GPR92. *J. Biol. Chem.* **283**, 21054–21064 (2008).
18. Alderton, F., Sambi, B., Tate, R., Pyne, N.J. & Pyne, S. Assessment of agonism at G-protein coupled receptors by phosphatidic acid and lysophosphatidic acid in human embryonic kidney 293 cells. *Br. J. Pharmacol.* **134**, 6–9 (2001).
19. Zhang, H. *et al.* Dual activity lysophosphatidic acid receptor pan-antagonist/autotaxin inhibitor reduces breast cancer cell migration in vitro and causes tumor regression in vivo. *Cancer Res.* **69**, 5441–5449 (2009).

20. Bang, S., Yoo, S., Yang, T.J., Cho, H. & Hwang, S.W. Farnesyl pyrophosphate is a novel pain-producing molecule via specific activation of TRPV3. *J. Biol. Chem.* **285**, 19362–19371 (2010).
21. Cohen, A., Sagron, R., Somech, E., Segal-Hayoun, Y. & Zilberberg, N. Pain-associated signals, acidosis and lysophosphatidic acid, modulate the neuronal K(2P)2.1 channel. *Mol. Cell. Neurosci.* **40**, 382–389 (2009).
22. Uehata, M. *et al.* Calcium sensitization of smooth muscle mediated by a Rho-associated protein kinase in hypertension. *Nature* **389**, 990–994 (1997).
23. Bourinet, E., Soong, T.W., Stea, A. & Snutch, T.P. Determinants of the G protein-dependent opioid modulation of neuronal calcium channels. *Proc. Natl. Acad. Sci. USA* **93**, 1486–1491 (1996).
24. Koch, W.J., Hawes, B.E., Inglese, J., Luttrell, L.M. & Lefkowitz, R.J. Cellular expression of the carboxyl terminus of a G protein-coupled receptor kinase attenuates Gβγ-mediated signaling. *J. Biol. Chem.* **269**, 6193–6197 (1994).
25. Chaytor, A.T., Edwards, D.H., Bakker, L.M. & Griffith, T.M. Distinct hyperpolarizing and relaxant roles for gap junctions and endothelium-derived H_2O_2 in NO-independent relaxations of rabbit arteries. *Proc. Natl. Acad. Sci. USA* **100**, 15212–15217 (2003).
26. Tang, L. *et al.* Antinociceptive pharmacology of *N*-(4-chlorobenzyl)-*N*′-(4-hydroxy-3-iodo-5-methoxybenzyl) thiourea, a high-affinity competitive antagonist of the transient receptor potential vanilloid 1 receptor. *J. Pharmacol. Exp. Ther.* **321**, 791–798 (2007).
27. Cenni, V. *et al.* Regulation of novel protein kinase C ε by phosphorylation. *Biochem. J.* **363**, 537–545 (2002).
28. Mintzer, E., Sargsyan, H. & Bittman, R. Lysophosphatidic acid and lipopolysaccharide bind to the PIP2-binding domain of gelsolin. *Biochim. Biophys. Acta* **1758**, 85–89 (2006).
29. Kumar, N., Zhao, P., Tomar, A., Galea, C.A. & Khurana, S. Association of villin with phosphatidylinositol 4,5-bisphosphate regulates the actin cytoskeleton. *J. Biol. Chem.* **279**, 3096–3110 (2004).
30. Klein, R.M., Ufret-Vincenty, C., Hua, L. & Gordon, S. Determinants of molecular specificity in phosphoinositide regulation. *J. Biol. Chem.* **283**, 26208–26216 (2008).
31. Yao, J. & Qin, F. Interaction with phosphoinositides confers adaptation onto the TRPV1 pain receptor. *PLoS Biol.* **7**, e46 (2009).
32. Prescott, E.D. & Julius, D. A modular PIP2 binding site as a determinant of capsaicin receptor sensitivity. *Science* **300**, 1284–1288 (2003).
33. Tominaga, M. *et al.* The cloned capsaicin receptor integrates multiple pain-producing stimuli. *Neuron* **21**, 531–543 (1998).
34. Inoue, M. *et al.* Lysophosphatidylcholine induces neuropathic pain through an action of autotaxin to generate lysophosphatidic acid. *Neuroscience* **152**, 296–298 (2008).
35. Ueda, H. Peripheral mechanisms of neuropathic pain—involvement of lysophosphatidic acid receptor-mediated demyelination. *Mol. Pain* **4**, 11 (2008).
36. Chemin, J. *et al.* Lysophosphatidic acid-operated K^+ channels. *J. Biol. Chem.* **280**, 4415–4421 (2005).
37. Kelly, J.J. Jr., Kyle, R.A., Miles, J.M. & Dyck, P.J. Osteosclerotic myeloma and peripheral neuropathy. *Neurology* **33**, 202–210 (1983).
38. Schwei, M.J. *et al.* Neurochemical and cellular reorganization of the spinal cord in a murine model of bone cancer pain. *J. Neurosci.* **19**, 10886–10897 (1999).
39. Marincsák, R. *et al.* Increased expression of TRPV1 in squamous cell carcinoma of the human tongue. *Oral Dis.* **15**, 328–335 (2009).
40. Renbäck, K., Inoue, M., Yoshida, A., Nyberg, F. & Ueda, H. Vzg-1/lysophosphatidic acid-receptor involved in peripheral pain transmission. *Brain Res. Mol. Brain Res.* **75**, 350–354 (2000).
41. García-Sanz, N. *et al.* A role of the transient receptor potential domain of vanilloid receptor I in channel gating. *J. Neurosci.* **27**, 11641–11650 (2007).
42. McIntyre, T.M. *et al.* Identification of an intracellular receptor for lysophosphatidic acid (LPA): LPA is a transcellular PPARγ agonist. *Proc. Natl. Acad. Sci. USA* **100**, 131–136 (2003).
43. Hama, K., Bandoh, K., Kakehi, Y., Aoki, J. & Arai, H. Lysophosphatidic acid (LPA) receptors are activated differentially by biological fluids: possible role of LPA-binding proteins in activation of LPA receptors. *FEBS Lett.* **523**, 187–192 (2002).
44. Salazar, H. *et al.* A single N-terminal cysteine in TRPV1 determines activation by pungent compounds from onion and garlic. *Nat. Neurosci.* **11**, 255–261 (2008).
45. Nishimasu, H. *et al.* Crystal structure of autotaxin and insight into GPCR activation by lipid mediators. *Nat. Struct. Mol. Biol.* **18**, 205–212 (2011).
46. Hausmann, J. *et al.* Structural basis of substrate discrimination and integrin binding by autotaxin. *Nat. Struct. Mol. Biol.* **18**, 198–204 (2011).
47. Karliner, J.S. Lysophospholipids and the cardiovascular system. *Biochim. Biophys. Acta* **1582**, 216–221 (2002).
48. Sams, H.H., Dunnick, C.A., Smith, M.L. & King, L.E. Jr. Necrotic arachnidism. *J. Am. Acad. Dermatol.* **44**, 561–573 (2001).
49. Caccin, P., Rigoni, M., Bisceglie, A., Rossetto, O. & Montecucco, C. Reversible skeletal neuromuscular paralysis induced by different lysophospholipids. *FEBS Lett.* **580**, 6317–6321 (2006).
50. Rosenbaum, T. & Gordon, S.E. Dissecting intersubunit contacts in cyclic nucleotide-gated ion channels. *Neuron* **33**, 703–713 (2002).

Acknowledgments

We thank D. Julius at University of California, San Francisco for providing the TRPV1 and TRPV2 cDNA, A. Patapoutian at the Scripps Research Institute for the TRPA1 cDNA, A. Toker at Harvard Medical School for PKCε dominant-negative and wild-type plasmids, J.A. García-Sáinz for his kind gift of BIM I and M. Calcagno for helpful discussion. We also thank L. Ongay, A. Escalante and F. Pérez at Instituto de Fisiología Celular, Universidad Nacional Autónoma de México (UNAM) for expert technical support and F. Sierra for expert help with DRG neuron culture. We are grateful to C.C. Durán and V.G. Soto for very valuable help with paw-withdrawal experiments. This work was supported by Dirección General de Asuntos del Personal Académico–Programa de Apoyo a Proyectos de Investigación e Innovación Tecnológica (DGAPA-PAPIIT) grant IN209209 and Instituto de Ciencia y Tecnología del Distrito Federal (ICYT-DF) grant PIFUTP09-262 to L.D.I., PAPIIT grants IN216009 and CONACyT 53777 to D.E.-A., and PAPIIT grants IN294111-3 and CONACyT CB-129474 and a grant from Fundación Miguel Alemán to T.R. This study was performed in partial fulfillment of the requirements for A.N.-P.'s doctoral degree in biomedical sciences at the UNAM.

Author contributions

A.N.-P., G.P.-J. and A.J.-O. performed electrophysiological experiments. I.L. carried out all site-directed mutagenesis. S.M.-L. performed all animal matings, genotyping and biochemical assays. D.E.-A., L.D.I. and T.R. jointly conceived the study, performed recordings and analysis, and wrote the paper.

Competing financial interests

The authors declare no competing financial interests.

Additional information

Supplementary information is available online at http://www.nature.com/naturechemicalbiology/. Reprints and permissions information is available online at http://www.nature.com/reprints/index.html. Correspondence and requests for materials should be addressed to T.R., D.E.-A. or L.D.I.

CORRIGENDUM

Lysophosphatidic acid directly activates TPRV1 through a C-terminal binding site

Andrés Nieto-Posadas, Giovanni Picazo-Juárez, Itzel Llorente, Andrés Jara-Oseguera, Sara Morales-Lázaro, Diana Escalante-Alcalde, León D Islas & Tamara Rosenbaum

Nat. Chem. Biol. **8**, 78–85 (2012); published online 20 November 2011; corrected after print 15 June 2012

In the version of this article initially published, the amount of LPA used in behavioral assays was incorrectly stated in the Methods section as 3 μg when it should have read 4.1 μg. Also, the details of preparation of LPA stock solutions were incomplete in the Methods section. The errors have been corrected in the HTML and PDF versions of the article.

CORRECTION NOTICE

Nat. Chem. Biol. **8**, 78–85 (2012)

Lysophosphatidic acid directly activates TPRV1 through a C-terminal binding site

Andrés Nieto-Posadas, Giovanni Picazo-Juárez, Itzel Llorente, Andrés Jara-Oseguera, Sara Morales-Lázaro, Diana Escalante-Alcalde, León D Islas & Tamara Rosenbaum

In the version of this supplementary file originally posted online, the amount of LPA used in behavioral assays was incorrectly stated in the legend of Supplementary Figure 1 as 3 μg when it should have read 4.1 μg. The error has been corrected in this file as of 15 June 2012.

Supplementary Information for

Lysophosphatidic acid directly activates TRPV1 through a C-terminal binding site

Andrés Nieto-Posadas, Giovanni Picazo-Juárez, Itzel Llorente, Andrés Jara-Oseguera, Sara Morales- Lázaro, Diana Escalante-Alcalde, León D. Islas, Tamara Rosenbaum

Supplementary Methods

Supplementary Results

Supplementary Methods

Reverse Transcription-PCR Analysis

Total RNA was isolated from mouse DRG neurons, Mouse Embryonic Fibroblasts (MEFs) and HEK293 cell lines with TRIZOL Reagent (Invitrogen). Two micrograms of total RNA were reverse transcribed with AMV reverse transcriptase (Promega) according to the manufacturer's instructions. The cDNA was amplified by PCR using the following primers: for mouse samples $mLPA_5$-S (5'-TGGCAGAGTCTTCTGGACACT-3') and $mLPA_5$-AS (5'-CCAAAGGC CTGGTATTCAGCG-3'); for human sample $hLPA_5$-S (5'- TAACCTCGTCA TCTTCCTGCT-3') and $hLPA_5$-AS (5'- TGTGAAGGAAGACAGAGAGTG-3'). The PCR cycling parameters were as follows: denaturation at 95 °C for 5 min followed by 30 cycles of denaturation at 95 °C for 30 s, annealing at 60 °C for 30 s, and extension at 72 °C for 45 s. PCR products were separated on a 1.5% agarose gel, stained with ethidium bromide, and photographed under a UV light source.

Treatments with G-protein coupled receptor (GPCR) signaling pathways inhibitors.

For experiments using GPCR-mediated signaling inhibitors, HEK293 cells were incubated over-night with Y27632 (260 μM for PKC and 10 μM for ROCK) and with bisindolylmaleimide I hydrochloride (BIM I, 1 μM); all from Calbiochem, USA. The phospholipase C inhibitor U-73122 (10 μM, Santa Cruz Biotechnology) and the adenylyl-cyclase inhibitor 2', 5'-dideoxyadenosine (500 μM, Sigma) were applied to HEK293 cells for 30 min. Finally, the βγ-subunits of the G-protein scavenger (Ctr-βARK1) was cotransfected with WT TRPV1. Currents were then recorded at 120 mV using the on-cell configuration of the patch-clamp technique and were first exposed to 4 μM capsaicin to obtain maximal-activation values. Then capsaicin was washed off and 5 μM LPA was added to obtain the fraction of current activated by this lipid. Data were compared to cells not incubated with the inhibitors. Epsilon –V1 – 2, epsilon – PKC Inhibitor, Cys – conjugated ($\varepsilon V_{1\text{-}2}$, ANASPEC) was diluted in water and delivered intracellularly to DRG neurons at a concentration of 200 μM via the recording electrode in whole-cell recordings.

Supplementary Results

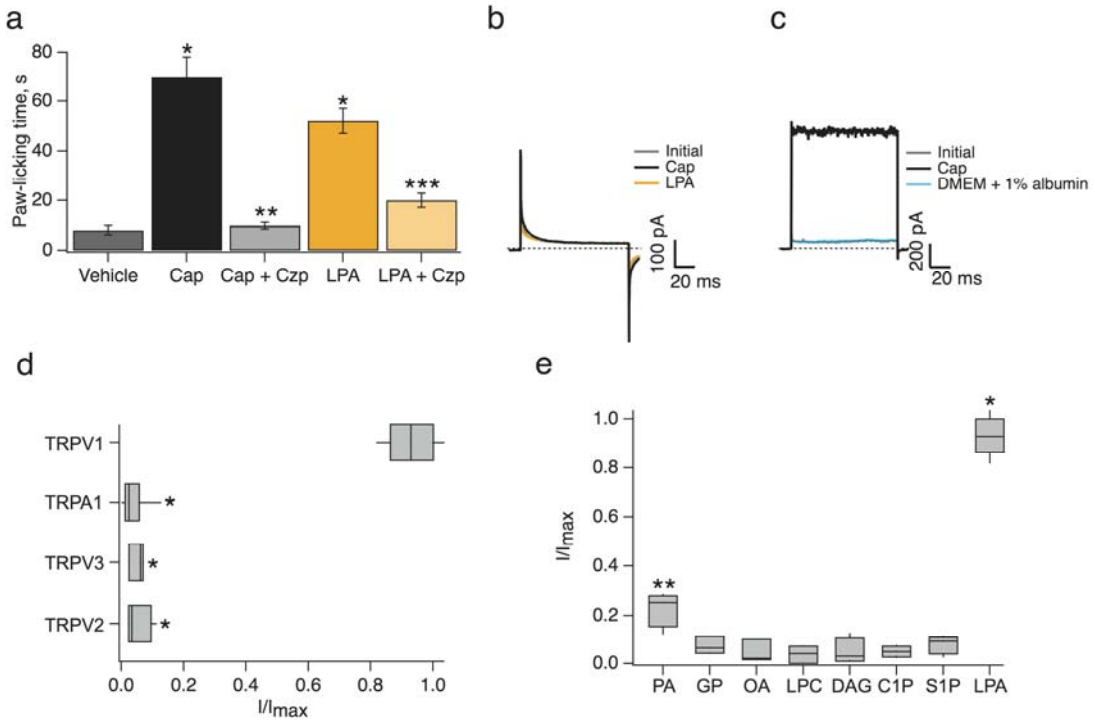

Supplementary Figure 1. Control experiments showing specificity of LPA actions on TRPV1.

(a) Coapplication of capsazepine (Czp) with LPA mimics the pain-like behavior of the TRPV1$^{-/-}$ upon LPA injection. Paw-licking time after injection of 2.8 μg of capsaicin was 70 ± 8 s vs 8 ± 1.8 s for saline and coinjection of capsaicin + Czp (2.2 μg) was 9.8 ± 1.3 s. Paw-licking time after injection of LPA (4.1 μg) was 52 ± 5 s and 20 ± 2.8 for LPA + Czp. *denotes $p < 0.01$ with respect to vehicle, ** $p < 0.01$ between capsaicin and capsaicin + Czp and *** $p< 0.01$ with respect to LPA and LPA+ Czp (n=10).

(b) GFP-transfected cells are not activated by capsaicin (black trace) nor LPA (orange trace) as compared to leak currents (grey trace) in inside-out membrane patches (120 mV). Representative traces from 5 experiments.

(c) The vehicle where LPA was diluted does no activate TRPV1 expressed in HEK cells. While capsaicin promotes current activation (black trace), currents measured in vehicle (DMEM + 1% fatty acid free-albumin, blue trace) behave like the initial currents (grey trace). Representative traces from 5 experiments for each case (inside-out membrane patches, 120 mV).

(d) TRPA1, TRPV2 and TRPV3 do not respond to LPA. The box-plot depicts the effects of LPA on TRP-channel activation. Data are expressed as the fraction of current in the presence of LPA normalized with respect to maximal activation with each channel´s known activator (30 μM 2-aminoethoxydiphenylborane (2-APB) for TRPV2 and 2mM for TRPV3, 400 μM allicin for TRPA1; 4 μM for TRPV1 which is the same data as in Figure 2b). The vertical line within each box indicates the median, boxes show the twenty-fifth and seventy-fifth percentiles, and whiskers show the fifth and ninety-fifth percentiles of the data (n = 5).

* * denotes a significant difference of $p < 0.01$ between TRPV1 and the other

channels, ANOVA test. All experiments were performed in the inside-out configuration of the patch clamp at 120 mV except with TRPA1, where the cell-attached configuration was used to avoid rundown.
(e) Box-plot depicting the effects of LPA-related molecules on the TRPV1. Phosphatidic acid (PA) produced a small but significant effect on TRPV1-current activation when compared to its own leak currents but glycerol phosphate (GP), oleic acid (OA), lysophosphatidylcholine (LPC), diacylglycerol (DAG), ceramide-1-phosphate (C1P) and sphingosine-1-phosphate (S1P) failed to promote channel activation. All molecules were applied at a concentration of 5 μM from the intracellular side of the membrane in TRPV1-expressing HEK-cell patches. Data are expressed as the fraction of current normalized with respect to maximal activation with saturating capsaicin (4 μM) at 120 mV. The horizontal line within each box indicates the median, boxes show the twenty-fifth and seventy-fifth percentiles, and whiskers show the fifth and ninety-fifth percentiles of the data (n = 6). * denotes a significant difference of $p < 0.01$ between LPA and the other compounds and ** denotes significance of $p < 0.05$ between PA and the rest of the lipids, ANOVA test.

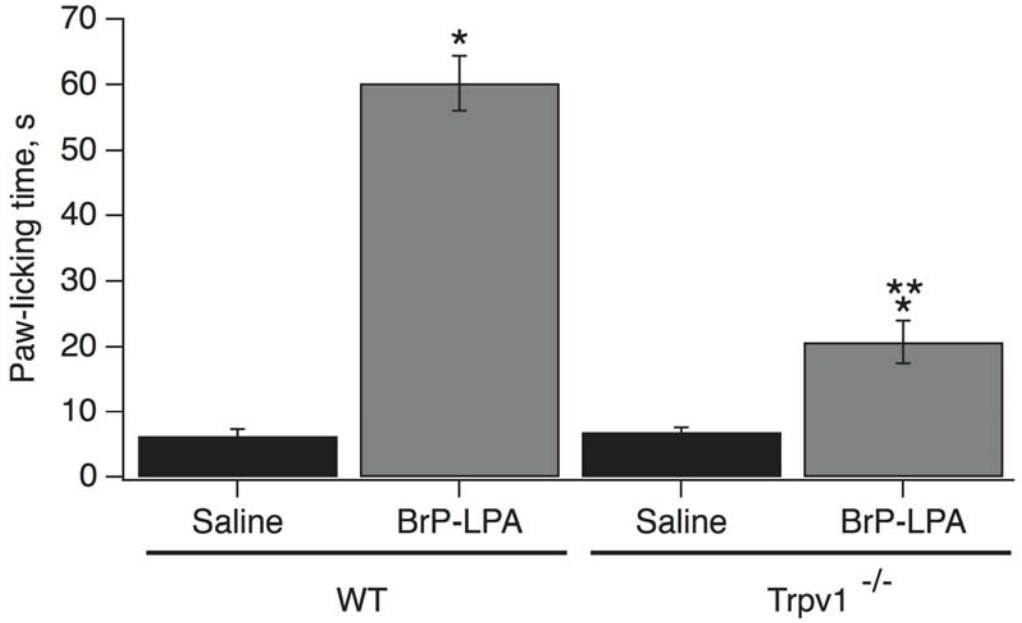

Supplementary Figure 2. BrP-LPA mimics the pain-like behavior induced by LPA. Paw-licking time after injection of 3μg BrP-LPA was 60 ± 4 s vs 6 ± 1 s for saline in control and 21 ± 3 s vs 7 ± 0.7 s for saline in *Trpv1*$^{-/-}$ mice. * denotes $p < 0.01$ between saline- and BrP-LPA- injected animals and **$p < 0.01$ between control and *Trpv1*$^{-/-}$ mice injected with BrP-LPA, ANOVA test. (n=12)

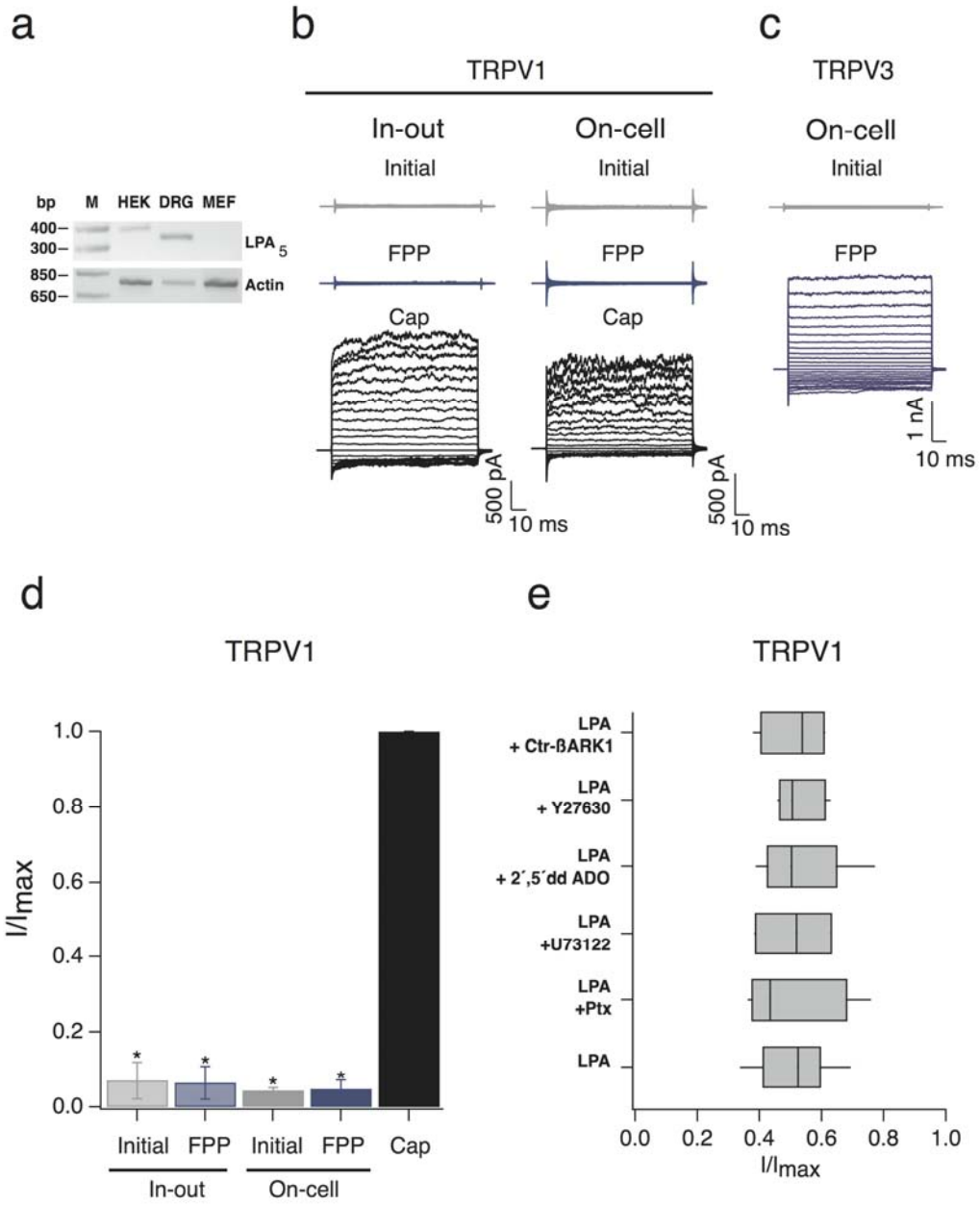

Supplementary Figure 3. LPA_5 is not involved in the response of TRPV1 to LPA.
(a) Lane 1 is the molecular weight marker. LPA_5 cDNA was amplified from reverse transcribed mRNA from HEK293 cells (lane 2), mouse DRG neurons (lane 3), and mouse embryonic fibroblasts (MEF, lane 4). Representative of 3 equal experiments.
(b) Representative current families obtained in the inside-out and on-cell configurations of the patch-clamp technique in response to voltage pulses from -120 to 120 mV in 10 mV increments (n= 5 for each configuration) using TRPV1-transfected HEK cells. Initial currents were first measured in the absence of any compound (grey, top), then in the presence of 1.5 μM FPP (blue, middle) and finally with 4 μM capsaicin (black, bottom).
(c) Representative traces in the on-cell configuration of 5 equal experiments from HEK293 cells expressing the TRPV3 channel. Initial currents were first obtained in the absence of any compound (grey, top) and then in the presence of 1.5 μM FPP (blue, bottom).
(d) Bar-chart for averaged data obtained from experiments shown in (b). For inside-

out experiments, the fractions of measured currents at 120 mV with respect to 4 μM capsaicin were: initial, 0.07 ± 0.04 and FPP, 0.06 ± 0.04. For on-cell experiments the fractions were: initial, 0.04 ± 0.007 and FPP, 0.04 ± 0.02. Data are expressed as mean ± s.e.m (n = 5 for each group).

(e) Box-plot of the fraction of current activated by LPA with respect to 4 μM capsaicin in the on-cell configuration after the incubation of cells with inhibitors of LPA receptor-associated signaling pathways (n = 5). The horizontal line within each box indicates the median, boxes show the twenty-fifth and seventy-fifth percentiles, and whiskers show the fifth and ninety-fifth percentiles of the data.

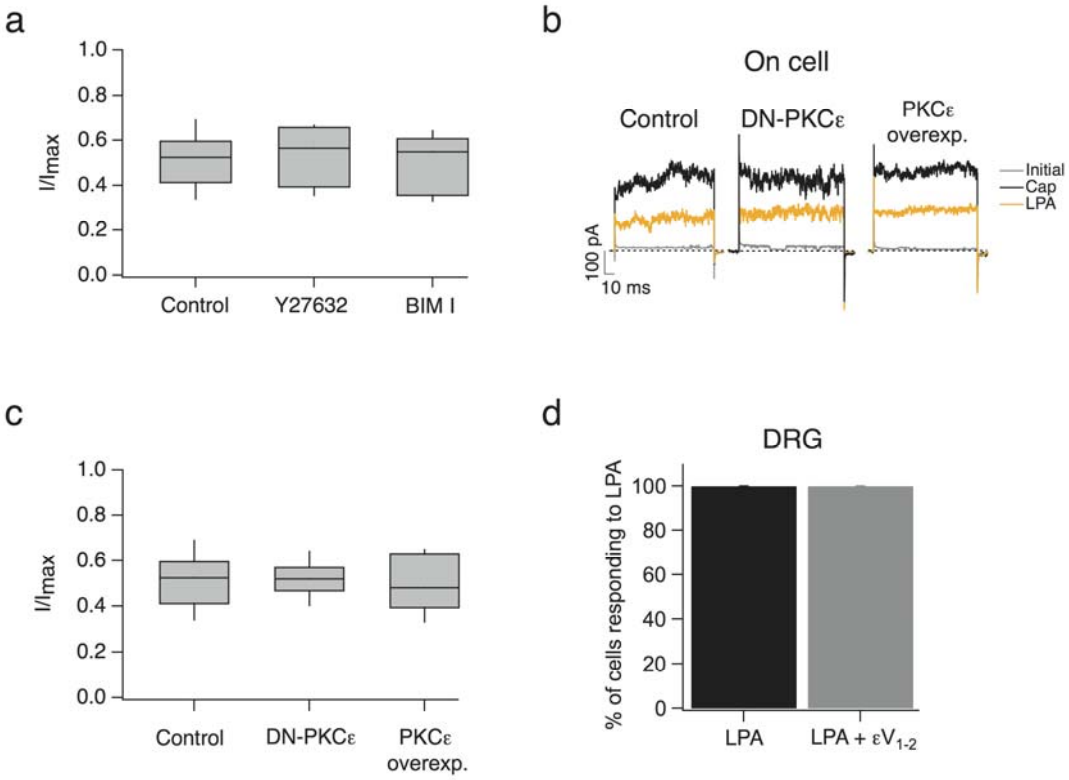

Supplementary Figure 4. PKCε is not involved in TRPV1 activation by LPA.
(a) PKC inhibitors do not abrogate LPA effects. Mean TRPV1-currents recorded in on-cell HEK-cell membrane patches elicited by 5 μM LPA at 120 mV after Y27632 (260 μM) or BIM I (1 μM) treatments and normalized to the mean current in saturating capsaicin. Box-plot content is as in Fig.2b (n = 6).
(b) Representative traces (n = 6) for activation of TRPV1 by LPA (on-cell) in a HEK293 cell expressing only TRPV1 (left) or TRPV1 and either the dominant negative PKCε (middle) or the WT PKCε (right) at 120 mV.
(c) Box-plot of the fraction of currents activated by LPA relative to 4 μM capsaicin for experiments as in (b).
(d) Percentage DRG neurons which responded to LPA with a TRPV1-like current with (left) or without the PKCε inhibitor $\varepsilon V_{1\text{-}2}$ in the pipette solution of whole-cell patches (-60 mV, n = 6).

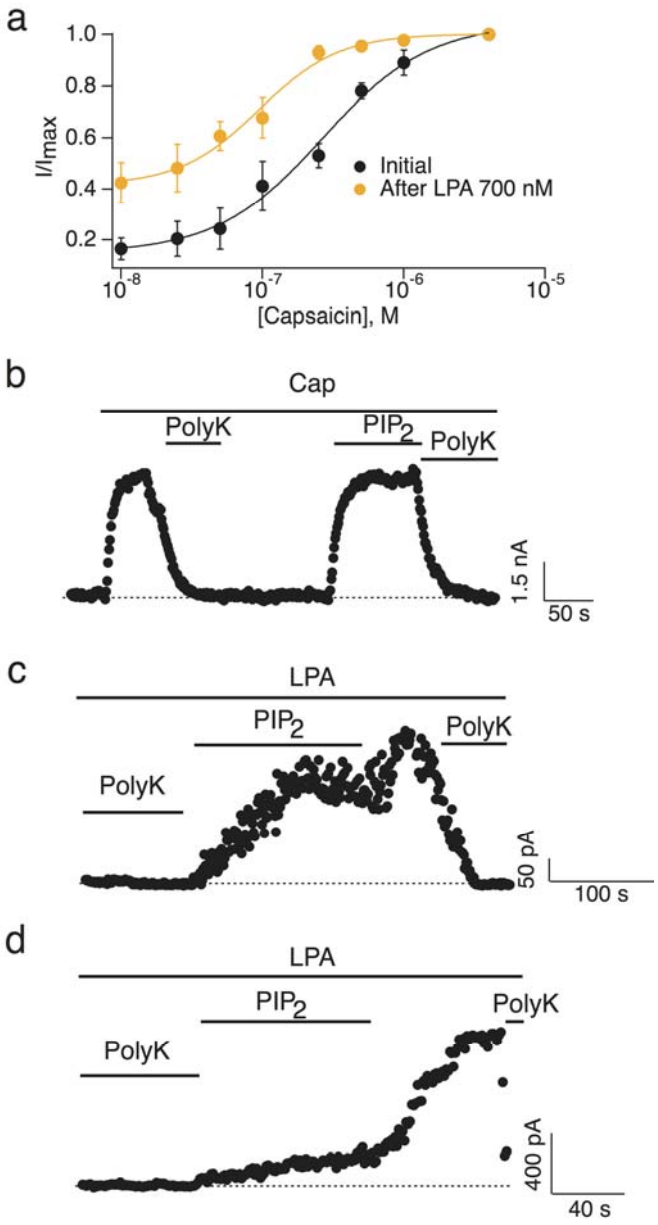

Supplementary Figure 5. Activation of TRPV1 in the presence of LPA and PIP_2.
(a) Additive effects of LPA and capsaicin on TRPV1 activation. Initial dose-response to capsaicin alone (K_D = 228 ± 85 nM and slope = 1. 3 ± 0.18; black symbols and black curve) and together with 700 nM LPA (K_D = 85 ± 32 nM and slope = 1.4 ± 0.23; orange symbols and orange curve) at 120 mV in inside-out membrane patches. Smooth curves are fits to the Hill equation. Pooled data are presented as mean ± s.e.m of 4 equal experiments.
(b) DiC8-PIP_2 inhibits the response of TRPV1 to LPA. Time-course of TRPV1-activation by capsaicin (100 nM), inhibition by polylysine (polyK) (15 μg/ml) and recovery by addition of DiC8-PIP_2 (200 nM) in inside-out membrane patches.
(c and d) Time-course of TRPV1-activation (+120 mV) by LPA (5 μM) exhibiting inhibition by polyK (15 μg/ml) and 50 nM (c) and (d) 200 nM DiC8-PIP_2 in the inside-out configuration. LPA was present throughout the whole experiment.

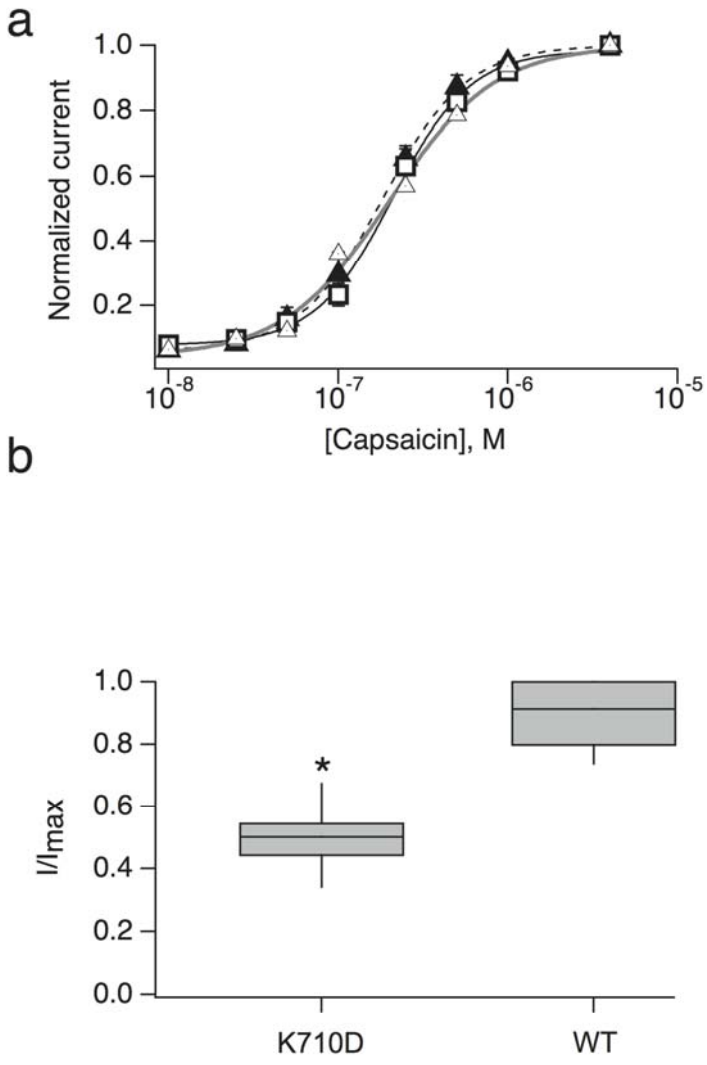

Supplementary Figure 6. Effects of BrP-LPA on the TRPV1-K710D channel.
(a) The response to capsaicin is not affected in the TRPV1-K710Q and TRPV1-K710D mutants. Dose-response curves to capsaicin of TRPV1-K710Q (K_D = 185 ± 6 nM: filled triangles and dotted curve) and of TRPV1-K710D (K_D = 246 ± 53 nM; empty triangles and grey curve) as compared to WT (228 ± 85 nM; squares and black curve) at 120 mV in inside-out membrane patches. Smooth curves are fits to the Hill equation. Pooled data are presented as mean ± s.e.m of 5 equal experiments.
(b) The K710D mutation abrogates BrP-LPA's effects on TRPV1 currents. Box-plot for the fraction of current activated by BrP-LPA (5 μM) in the TRPV1-K710D mutant as compared to WT and normalized with respect to currents activated by saturating capsaicin. The vertical line within each box indicates the median, boxes show the twenty-fifth and seventy-fifth percentiles, and whiskers show the fifth and ninety-fifth percentiles of the data. The symbol *denotes significance of $p < 0.01$, n =6, ANOVA test.

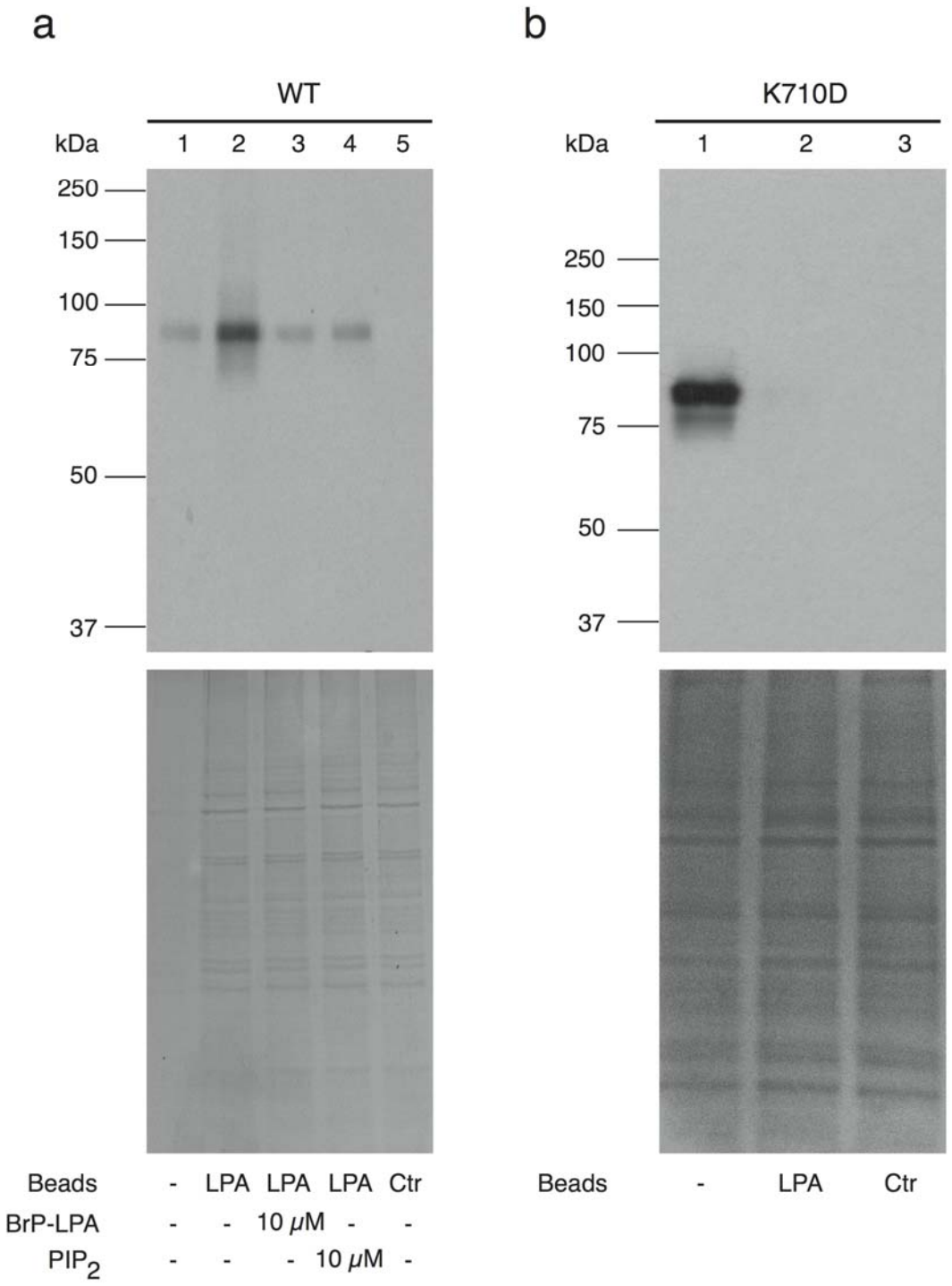

Supplementary Figure 7. Binding of TRPV1 to LPA-beads is specific.
(a) TRPV1 interaction with LPA-coated beads. Lane 1= input (1 μg), 2= TRPV1 bound to LPA-beads, 3 and 4= competition of BrP-LPA and PIP_2 for beads, respectively and 5= interaction with control beads. 2,3,4,5 contained 30 μg of membrane protein. Lower panel= Coomasie blue-stained supernatant fraction.
(b) Interaction of K710D with LPA-coated beads. Lane 1= the input (5 μg) of the TRPV1-K710D mutant, 2= pull-down of TRPV1-K710D with LPA-beads and 3= control beads. 2 and 3 contain 60 μg of membrane protein. Lower panel= Coomasie blue-stained supernatant fraction.